Droplet Charging Effects in the Space Environment

Thomas B. Joslyn[a] and Andrew D. Ketsdever[b]

[a]*United States Air Force Academy, Department of Astronautics, USAF Academy, CO 80840*
[b]*University of Colorado at Colorado Springs, Department of Mechanical and Aerospace Engineering, Colorado Springs, CO 80918*

Abstract. Several applications exist for transiting liquid droplets through the near-Earth space environment. Numerical results are presented for the charging of liquid droplets of trimethyl pentaphenyl siloxane (DC705) in three different plasma environments: ionosphere, auroral, and geosynchronous Earth orbit (GEO). Nominal and high geomagnetic activity cases are investigated. In general, high levels of droplet charging (>100V) exist only in GEO during periods of high geomagnetic or solar activity. An experiment was conducted to assess the charging of silicon-oil droplets due to photoemission. The photoemission yield in the 120-200nm wavelength range was found to be approximately 0.06.

Keywords: liquid droplet charging, plasma environment.
PACS: 52.65.-y, 94.05.Sd

INTRODUCTION

The idea of propagating liquid droplet streams through the space environment was first put forth in the 1980s as a means of spacecraft thermal control.[1] These liquid droplet radiator concepts release multiple liquid droplet streams into space where the droplets radiate heat. The cooled liquid droplets are collected on the same spacecraft after a short distance, pumped throughout the spacecraft to remove heat from various components, and released back into space to cool again.. A subsequent study has alluded to other potential applications for liquid droplets transiting the near-Earth space environment.[2] For the application of interest in this study, a liquid droplet stream of low-vapor-pressure, silicon-based oil is being proposed as a potential spacecraft propulsion system.[3] In this concept, liquid droplets are constantly passed between two (or multiple) spacecraft flying in formation. The receiving satellite collects the liquid droplet stream from the originating satellite and returns the liquid droplets back to the original satellite. This "pitch and catch" scenario allows a constant momentum exchange between the two satellites allowing a constant spacing to be maintained between the spacecraft. Large arrays of satellites can be envisioned using this concept where the relative spacing between individual satellite members of the array can be constantly controlled.

Trimethyl pentaphenyl siloxane (better known by its trade name of DC 705) was selected as the liquid of choice due to its low-vapor-pressure and viscosity. Obviously, the low-vapor-pressure is required for the liquid droplet to be appropriate for a space application. The low viscosity allows the fluid to be transported throughout the spacecraft at relatively little pumping power.

An object in near-Earth space is subject to many interactions with the ambient environment at a given altitude such as exposure to atomic oxygen, radiation, and charged particles.[4] This study investigates the interactions between the ambient, near-Earth plasma environment and DC 705 liquid droplets. Charging of the DC 705 can cause operational concerns for all of the space related applications discussed above. Since DC 705 is a dielectric material, differential charging can cause a droplet to breakup if the Coulomb repulsive force is greater than the surface tension force holding the droplet together. Also, for this particular application, a stream of charged droplets in close proximity can begin to produce Coulomb-type forces between individual droplets potentially leading them off course.

This study assesses the charging potential of DC 705 in three general near-Earth environments as a function of geomagnetic and solar activity using a numerical approach. An experiment was designed to quantify the amount of droplet charging due to solar extreme ultraviolet (EUV) radiation exposure, one of several mechanisms that can cause droplet charging in space.

THEORY

As objects move through space, they come into contact with ambient ions and electrons that constitute the Earth's plasma environment. Several different mechanisms are responsible for adding or removing electrons (charge) from an object exposed to a plasma environment. Quantifying the net current of an object immersed in a plasma is generally an iterative (i.e. numerical) process since the charge of the object is highly coupled to the plasma interaction mechanisms. The current balance for an object floating at an electrostatic potential, V, is given by

$$I_{net}(V) = I_e(V) - \{I_i(V) + I_{se}(V) + I_{si}(V) + I_{bse}(V) + I_{ph}(V)\} \quad (1)$$

where I_{net} is the net current flow to the object, I_e is the incident electron current, I_i is the incident ion current, I_{se} is the secondary electron current caused by the incident electrons, I_{si} is the secondary electron current caused by the incident ions, I_{bse} is the current caused by backscattered incident electrons, and I_{ph} is the secondary electron current caused by incident solar photons. In order to assess the charging of an object in a plasma environment, characteristics of the plasma environment (e.g. species, density and energy) and active plasma-surface interaction mechanisms must be understood.

Characteristics of the Plasma Environment

In general, the Earth's plasma environment can be separated into three main categories based on the characteristics (e.g. density and energy) of the ambient plasma species: ionosphere, auroral, and geosynchronous Earth orbit (GEO). The ionosphere ranges from an altitude of 100 km to approximately 1000 km. It is characterized by a relatively dense number density of heavy ion species dominated by O^+ between 150 and 900 km. Ion and electron number densities vary from approximately $7x10^5$ to 10^4 cm^{-3} over this altitude range. There is a reasonable degree of non-equilibrium in the ionosphere between neutral species, ions and electrons where the neutral temperature is essentially constant at approximately 1000K, the ion temperature varies from 1000 to 2000K, and the electron temperature varies from 1600 to 3200K.[4]

The auroral plasma environment is characterized by the high energy electrons precipitating down the Earth's magnetic field lines at high latitudes where solar wind electrons can readily access the upper atmosphere. The electron energy distribution in the auroral region is highly non-equilibrium as described by Fontheim et al.[5] The energy generally ranges from 0.1 to 10keV with higher energy particles generally having a lower flux. The electron density and energy in this region can be highly variable and can be influenced by solar and geomagnetic storms.[4] The GEO plasma environment is characterized by low density (~1cm^{-3}), high energy (0.6 to 20keV) electrons and protons. The GEO plasma environment is also highly variable.

Space Charging Mechanisms

The general charging mechanisms for an object in a moderate energy (<20keV) plasma environment are shown in Fig. 1. Secondary electrons formed from the interaction of ions, electrons, or photons on the surface may escape the material, be conducted through the material, or be re-adsorbed by the material. As can be deduced from Eq. 1, determining the total number of secondary electrons produced and accurately assessing the relative number that escape the material is critical in quantifying the material's charge state. In general, secondary electron yield (the average number of secondary electrons produced per incident collider) is a function of the incident collider (ion, electron, neutral, photon), the relative energy, and the material substrate. Secondary electron yields for DC 705 for electron and photon colliders have been experimentally determined by Ishikawa and Goto[6] and Koizumi et al.[7] respectively. Plots of the secondary electron yields for both electron and photon colliders with DC 705 are shown in Fig. 2 as a function of incident energy.

NASCAP MODEL

The NASA Charging Analyzer Program (NASCAP)[8] was used to quantify the charging of a DC 705 droplet exposed to the three space plasma environments described in the previous section. The potential in the plasma near a charged surface with potential V is given by the Poisson equation as

$$\epsilon_o \nabla^2 V = q(n_i - n_e) \quad (2)$$

where ϵ_o is the permittivity of free space, q is the elemental charge, and n_i and n_e are the number density of ions and electrons, respectively. NASCAP solves Eq. 2 by applying the specified environmental flux distribution of ions, electrons, and photons in an iterative process alternating the development of a plasma sheath at the surface and the recalculation of the near-surface plasma densities. NASCAP employs the Boundary Element Method which relates the electric fields in the surrounding plasma to sources at the surface. This method allows rapid determination of changes in plasma densities, current flow to and from the surface, and a new solution to Poisson's equation to determine changes in electrostatic potential that occur during the time step.

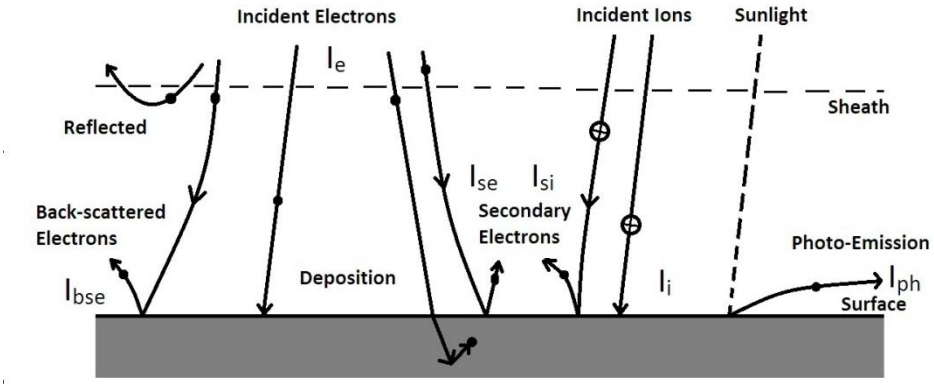

FIGURE 1. Charging Processes Near the Surface of a Dielectric Material.

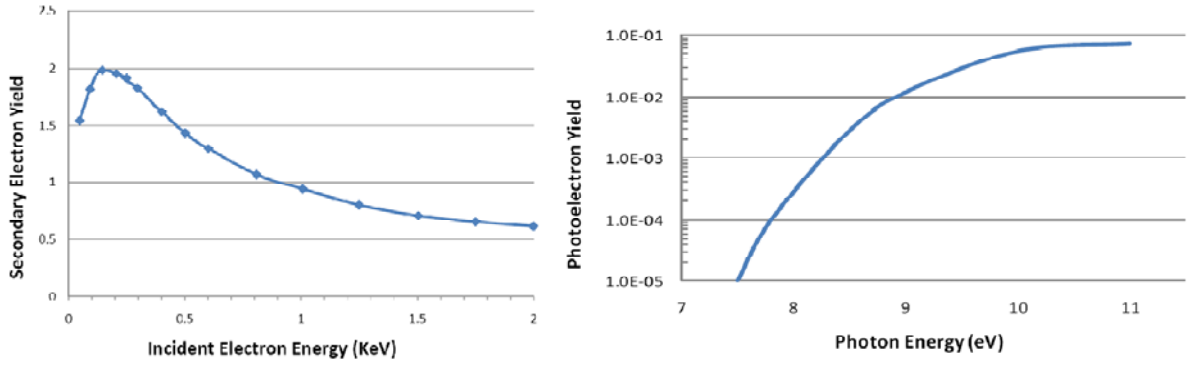

(A) **(B)**

FIGURE 2. Secondary Electron Yield as a Function of Energy for **(A)** Electron[6] and **(B)** Photon[7] Colliders at Normal Incidence.

Ionospheric environmental conditions are derived from data in the International Reference Ionosphere (IRI) model.[9] Auroral environmental conditions based on data from the Defense Meteorological Satellite Program (DMSP) were used.[5] Nominal and worst-case environments are derived from over 35 years of DMSP measurements orbiting at altitudes between 500 and 800km. The GEO environmental conditions are modeled after data from the Applications Technology Satellite (ATS) and the Spacecraft Charging at High Altitude (SCATHA) spacecraft.[10] Nominal and worst-case conditions are both modeled.

EXPERIMENTAL SET UP

An experiment was constructed to quantify DC704 charging due to photon colliders. DC704 is expected to have the same charging characteristics of DC705.[6] A continuous stream of DC704 droplets were produced in a small vacuum chamber and exposed to a 30W EUV lamp made by the Hamamatsu Corporation. The lamp, which was used to simulate the EUV output from the sun, emits photons in the wavelength range of 120 to 200nm using a deuterium plasma source. The spectral profile of the lamp can be found in ref. 3. The lamp position was varied relative to the droplet stream to change the irradiance at the droplet. After illumination by the solar simulator, the droplets passed through a parallel plate capacitor. The amount of deflection of the droplets in the parallel plate

capacitor is proportional to their charge. By measuring the deflection for a known droplet diameter (i.e. mass), the droplet charge due to secondary electrons produced by photon colliders was determined. The experimental set up is shown in Fig. 3.

In this set up, the droplets are only exposed to the EUV radiation as they fall through the opening of the cylindrical shield. Because the amount of charge built up on the droplets is a function of exposure time to the EUV radiation, the shield is meant to block the EUV from the droplet stream except for a well quantified amount of time. In these experiments, the exposure time is 0.065 sec.

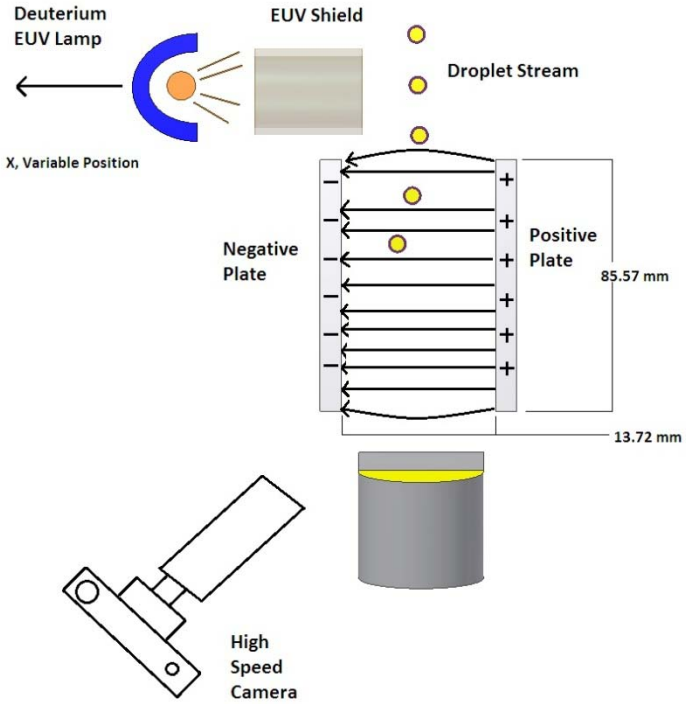

FIGURE 3. Photoemission Experimental Set Up.

RESULTS

Numerical

In general, differences in the charging in all three plasma environments considered are seen between droplets in the sun and those in eclipse. There are two main reasons for these differences. First, in eclipse, photoemission of secondary electrons from a surface is not an active mechanism for charge production. Second, there can be differences in the plasma environment between regions in the sun and those in eclipse. For example, the production of charged particles in the ionosphere is dominated by photo-ionization of neutral species. Diffusion and induced drifts cause the charged particles to be present in the eclipse region; however, there is a strong diurnal variation in density where some ionospheric layers (e.g. the D and F1 regions) completely disappear at night.[4] A summary of the charging on DC 705 droplets exposed to the three plasma environments is shown in Table 1. Values are given for both sunlit and eclipsed regions. The maximum charge found in the NASCAP simulations for any surface exposed to the sun is shown along with the minimum charge found on any surface during eclipse.

The nominal and high geomagnetic activity environments for the ionosphere show very benign charging characteristics for DC 705. For the nominal environment in sunlight, DC 705 reached a very small, nearly uniform negative charge potential of -0.01V relative to the ambient plasma potential. In eclipse, the surface potential was approximately -0.05V. These results are consistent with the idea that in a quasi-neutral plasma, a floating surface will charge slightly negative due to the fact that at the same energy the mean electron speed is higher (i.e. higher flux of electrons to the surface). The high geomagnetic environment in the ionosphere was also found to be fairly benign. Because of the relatively high density of both positively and negatively charged particles in the ionosphere,

any large potential built up on the droplet is quickly neutralized by collecting oppositely charged particles from the plasma.

The auroral environment simulations are highly dependent on the assumed plasma densities and energy distributions. At orbital speeds, the leading surface of a droplet (RAM direction) collects both ions and electrons. However, the trailing surface (anti-velocity vector or wake) only collects the much faster electrons (i.e. the speed of the droplet is much larger than the average thermal speed of the ions). Therefore, there are some slight differences in the charging of RAM and wake surfaces. At altitudes below 800km, the plasma densities are still relatively high and the sheath is fully developed within 0.5 sec.

Simulations for GEO are highly dependent on geomagnetic activity and photoemission. The strong dependence on droplet charge of photoemission can be seen in the difference of potential in the sunlight case versus the eclipse case in Table 1. In GEO, the orbital speed is such that it is less than the mean speed of both the electrons and ions. Because the ambient plasma density in GEO is extremely small ($n \sim 1 cm^{-3}$), the droplet can charge to extremely high negative potentials due to the increase in electron density during high geomagnetic or solar activity. In nominal environmental conditions, photoemission is the dominant charge mechanism which can lead to relatively high positive potentials.

TABLE (1). Summary of equilibrium charging results from NASCAP for various plasma environments. Maximum sunlit surface and minimum eclipsed surface values are given.

Environment	Ionosphere	Auroral (<800km)	GEO
Nominal Geomagnetic	0V, -1V	+4V, -16V	+18V, +1.5V
High Geomagnetic	+2V, -2V	+21V, -26V	-2kV, -13kV

Experimental

Figure 4 shows the average droplet charge potential as a function of the EUV lamp irradiance (normalized by the solar irradiance). The droplet potential is seen to vary linearly with the irradiance as expected. The experiment did not include an ambient plasma environment. Therefore, the droplets charge to relatively high positive potentials due to photoemission of secondary electrons without the opportunity to collect electrons from an ambient plasma to help neutralize the droplet charge. NASCAP simulations were run where the only active charging mechanism was photoemission (i.e. the background plasma was turned off). A study was conducted with the photoemission yield as the only parametric variable. Figure 5 shows the comparison of the transient NASCAP simulations with the experimental results. The numerical results show excellent agreement for a photoemission yield of 0.06. The empirical results for photoemission yield from DC704 and DC705 of Koizumi et al.[7] is shown in Fig. 6 along with the solar spectra and the assumed (i.e. provided by the manufacturer) spectra from the EUV lamp. The total irradiance is taken as the area under each spectra. As shown in Fig. 6, the EUV lamp used in this study should produce a photoemission yield somewhere between 0.03 and 0.06 of its range of transmission wavelengths which is consistent with the NASCAP results from Fig. 5.

CONCLUSIONS

In general, high levels of droplet charging (>100V) were only found in GEO during periods of high geomagnetic activity. Nominal GEO conditions along with conditions in the ionosphere and auroral environments tend to lead to levels of charging between +20V and -30V. The ambient plasma plays a dominant role in both the ionosphere and auroral environments. Generally, solar EUV radiation plays a dominant role in GEO during nominal environmental conditions. The effects of charging on DC705 droplets were found to be negligible in all cases except the high geomagnetic activity GEO scenario. The photoemission yield of approximately 0.06 found through a combination of experimental and numerical studies is consistent with the yields found in the literature for EUV wavelengths between 120 and 200nm.

ACKNOWLEDGMENTS

The authors wish to thank the United States Air Force Research Laboratory, Propulsion Directorate (Edwards AFB, California) for their support of this research. The figure-making skills of Mr. Ryan Bosworth are appreciated.

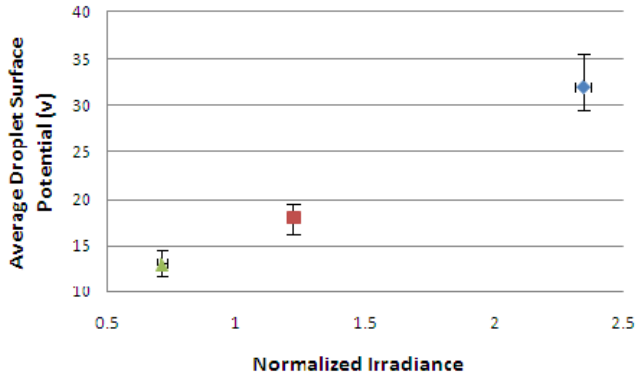

FIGURE 4. DC704 Droplet Potential as a Function of Normalized Irradiance (1=Solar Irradiance).

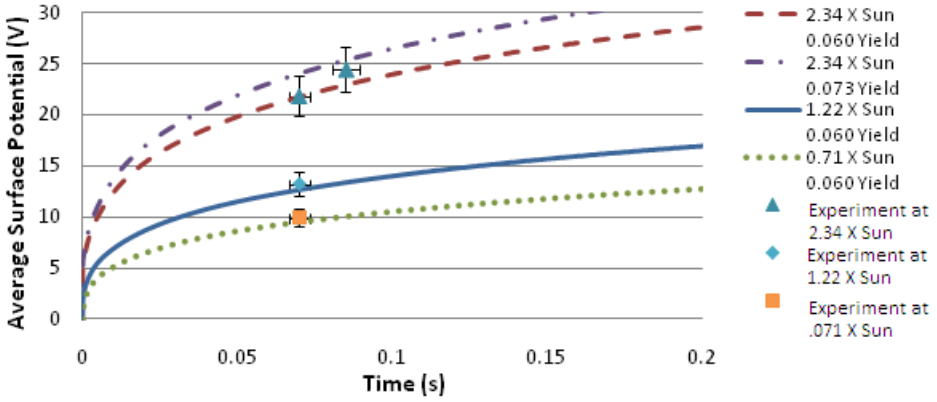

FIGURE 5. Comparison of NASCAP and Experimental Charging Results.

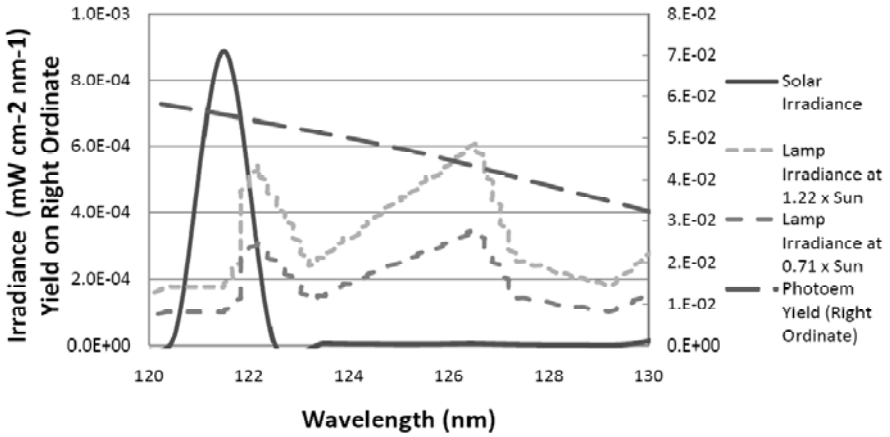

FIGURE 6. Typical Solar and EUV Lamp Irradiance with Corresponding Photoemission Yield (right ordinate).

REFERENCES

1. A. Mattick and A. Hertzberg. *J. Energy*, **5**, 387-393 (1981).
2. E.P. Muntz and M. Dixon, *J. Spacecraft Rockets*, 23, 411-419 (1986).
3. T. Joslyn, "Charging Effects on Fluid Stream Droplets for Momentum Exchange Between Spacecraft," Ph.D. Thesis, University of Colorado at Colorado Springs, 2009.
4. T. Gombosi, Physics of the Space Environment, Cambridge UK, Cambridge University Press, 1998.
5. E. Fontheim, K. Stasiewicz, and M. Chandler. *J. Geophys. Res.*, **87**, 3469-3480 (1982).
6. K. Ishikawa and K. Goto, *Jpn. J. Appl. Phys.*, **6**, 1329-1335 (1967).
7. H. Koizumi, K. Lacmann, and W. Schmidt. *IEEE Trans. Dielect. and Elect. Insul.*, **3**, 233-236 (1996).
8. M. Mandell, I. Katz, J. Hilton, J. Minor, and D. Cooke. *AIAA paper 2001-0957,* 39th Aerospace Sciences Meeting (2001).
9. C. Purvis, H. Garrett, A. Whittlesey, and N. Stevens. *NASA Technical Paper 2361* (1984).